



Research Article

ISSN : 0975-7384
CODEN(USA) : JCPRC5

Medical DR image alignment based improved tangent space

Zuo Weiming and Li Tie

Department of Computer Science, Hunan City University, China

ABSTRACT

Tangent space alignment is efficient in machine learning. This is about mapping several datasets into a global space, and is of great importance in learning the shared latent structure, data fusion and multicue data matching. In this paper, we propose an improved tangent space algorithm to solve medical DR image alignment problem. This algorithm builds the inner linear manifold constraint in Medical DR image. A cost function to measure the quality of alignment is given by combining the inner manifold constraints of each dataset and the matching points constraints among different datasets. The effectiveness of our algorithm is validated by applying it to the medical DR image alignment.

Keywords: Medical DR image, Local tangent space, Data analysis, Manifold learning

INTRODUCTION

Digital radiography (DR) has advantages, such as high resolution ratio, wide dynamic range, fast speed of imaging and low-radiation to human body. It uses a flat plate detector to accept the X-ray and obtains the digital image signal directly. It has been the most advanced medical imaging method in the X-ray imaging field, and more and more widely used in the clinical diagnosis and the scientific research. Recently, manifold alignment methods have attracted much attention in computer and pattern recognition. This question arises when one needs to find common structure or establishes a correspondence between two data sets resulting from the same fundamental source. For instance, consider the problem of matching pixels of a stereo image pair. One can form a graph for each image, where pixels constitute the nodes and where edges are weighted according to the local features in the image. The problem now boils down to matching nodes between two manifolds. Note that this situation is an instance of multisensor integration problem, in which one needs to find the correspondence between data captured by different sensors. In some applications, like fraud detection, synchronizing data sets is used for detecting discrepancies rather than similarities between data sets. There has been a body of work related to graph-based manifold alignment. Bai et al.[5] presents that the ISOMAP algorithm is used to embed the nodes of the graphs corresponding to the aligned data sets, in a low-dimensional Euclidean space. The nodes are thus transformed into points in a metric space, and the graph-matching is recast as the alignment of point sets. A variant of the Scott and Longuet-Higgins algorithm is then used to find point correspondences. Ham et al.[1] align the manifolds by giving a set of a priori corresponding nodes or landmarks. A constrained formulation of the graph Laplacian based embeddings is derived by including the given alignment information. First, they add a term fixing the embedding coordinates of certain samples to predefined values. Both sets are then embedded separately, where certain samples in each set are mapped to the same embedding coordinates. Second, they describe a dual embedding scheme, where the constrained embeddings of both sets are computed simultaneously, and the embeddings of certain points in both data sets are constrained to be identical. Gori et al.[6] align weighted and unweighted graphs by computing a “signature” for each node that is

based on repeated use of the invariant measure of different Markov chains defined on the data. The nodes/samples are then matched in two ways: First, in a one-by-one basis, where nodes with similar signatures are coupled. Second, in a globally optimal approach using a bipartite graph matching scheme. An approach to Many-to-Many alignment was presented in [7] by Keselman et al. They aim to match corresponding clusters of nodes in both data sets, rather than match individual nodes. The data sets are embedded in a metric space using the Matousek embedding and sets of nodes are then aligned using the Earth Mover's Distance, which is a distribution-based similarity measure for sets. In the data alignment segment of our work, we resolve the alignment of data sets with a common low-dimensional manifold, but different densities, by incorporating the use of the density-invariant embedding.

Manifold constraint of a single dataset

The basic idea of LTSA is to construct local linear approximations of the manifold in the form of a collection of overlapping approximate tangent spaces at each sample point, and then align those tangent spaces to obtain a global parametrization of the manifold. Details and derivation of the algorithm can be found in [4]. Given a data set $X = [x_1, \dots, x_N]$ with $x_i \in R^m$, sampled (possibly with noise) from a d -dimensional manifold ($d \ll m$), $x_i = f(\tau_i) + \varepsilon_i$, where $f: \Omega \subset R^d \rightarrow R^m$, Ω is an open connected subset, and ε_i represents noise. LTSA assumes that d is known and proceeds in the following steps.

(1) Local neighborhood construction. For each x_i , $i = 1, \dots, N$, determine a set $X_i = [x_{i_1}, \dots, x_{i_k}]$ of its neighbors (k nearest neighbors, for example).

(2) Local linear fitting. Compute the optimal rank- d approximation to the centered matrix $(X_i - \bar{x}_i e^T)$, where $\bar{x}_i = \frac{1}{k} \sum_{j=1}^k x_{i_j}$, and e is a k -dimensional row vector of all 1's. By the SVD of $X_i - \bar{x}_i e^T$, $X_i - \bar{x}_i e^T = Q \Sigma V^d$, if $\Sigma_d = \text{diag}(\sigma_1, \dots, \sigma_d)$ with the d largest singular value of $X_i - \bar{x}_i e^T$, Q_d and V^d are the matrices of correlating left and right singular vectors, respectively. we can obtain the orthonormal basis Q_i for the d -dimensional tangent space of the manifold at x_i , and the orthogonal projection of each x_{i_j} in its neighborhood to the computed tangent space $\theta_j^{(i)} = Q_i^T (x_{i_j} - \bar{x}_i)$.

(3) Local coordinates alignment. Align the N local projections $\Theta_i = [\theta_1^{(i)}, \dots, \theta_k^{(i)}]$, $i = 1, \dots, N$, to obtain the global coordinates. Denote τ_1, \dots, τ_N , and $T_i = [\tau_{i_1}, \dots, \tau_{i_k}]$ which consists of a subset of the columns of T with the index set $\{i_1, \dots, i_k\}$ determined by the neighbors of each x_i . Let $E_i = T_i - c_i e^T - L_i \Theta_i$ be the local reconstruction error matrix, where $c_i = \frac{1}{k} T_i e$ and $L_i = T_i (I - \frac{1}{k} e e^T) \Theta_i^+ = T_i \Theta_i^+$, where Θ_i^+ is the Moore-Penrose generalized inverse of Θ_i and e is a vector of all ones.

$$E_i = T S_i W_i \quad (1)$$

Where S_i is the 0-1 selection matrix such that $T S_i = T_i$ and $W_i = (I - \frac{1}{k} e e^T) (I - \Theta_i^+ \Theta_i)$. Then the single data set manifold alignment of LTSA is achieved by minimizing the following global reconstruction error:

$$E(T) = \sum_i \|E_i\|^2 \equiv \sum_i \|T S_i W_i\|_F^2 = \|T S \widehat{W}\|_F^2 \quad (2)$$

Where $S = [S_1, \dots, S_N]$ and $\widehat{W} = \text{diag}(W_1, \dots, W_N)$

Both the approximation vector w_i and the approximation matrix w_i are distilled from the high-dimensional data X . There are several methods to determine the approximation coefficients listed in Table 1. Local learning regularization and LLE[6] are two ways to determine the approximation vector w_i for the point mode. LTSA[7] offers us a method to determine the approximation matrix w_i for the block mode. Here θ_i is the mapping of \bar{X}_{Γ_i} in the local tangent space, θ_i^+ is the Moor-Penrose generalized inverse of θ_i , and $W_i = \theta_i^+ \theta_i$ acts like a correlation matrix of the points around x_i .

Medical DR Image Alignment Based Improved Tangent Space

Let Γ_i be a vector of indices of points in the $(k-1)$ -neighbor of x_i , and $\bar{\Gamma}_i = \begin{bmatrix} i \\ \Gamma_i \end{bmatrix}$ is a vector including i and Γ_i . S_i is a 0-1 selection matrix satisfying $XS_i = X_{\bar{\Gamma}_i}$. Similarly in the low-dimensional space, we have $YS_i = Y_{\bar{\Gamma}_i}$.

Let e be the vector of all 1's, I_k be the identify matrix with rank k . Then, $J = (I - \frac{1}{k}ee^T)$ is the mean removal operator. We can get the local coordinate of the high-dimensional data $\bar{X}_{\bar{\Gamma}_i} = X_{\bar{\Gamma}_i}J$, and its counterpart in low-dimension $\bar{Y}_{\bar{\Gamma}_i} = Y_{\bar{\Gamma}_i}J$. The approximation of a point is defined as $\bar{Y}_{\bar{\Gamma}_i}w_i \rightarrow \bar{Y}_i$, where w_i is the local approximation vector extracted from X .

The block approximation is defined as $\bar{Y}_{\bar{\Gamma}_i}W_i \rightarrow \bar{Y}_i$, where W_i is the local approximation extracted from points around x_i . The block approximation error around y_i is defined as $err_{bi} = \|\bar{Y}_{\bar{\Gamma}_i} - \bar{Y}_{\bar{\Gamma}_i}W_i\|_F^2 = \|YS_iJ(I_k - W_i)\|_F^2$. The summation of the approximation error of all local blocks is

$$err_b = \sum_{i=1}^n err_{bi} = \sum_{i=1}^n \|YS_iJ(I_k - W_i)\|_F^2 = \|YS_bB_b\|_F^2 \quad (3)$$

where $S_b = [S_1, \dots, S_n]$, $B_b = \text{diag}\{J(I_k - W_1), \dots, J(I_k - W_n)\}$.

Learning with the label value can be regarded[8] as the problem of approximating a multivariate function from labeled data points. The function can be real valued as in regression or binary valued as in classification. Learning with the label value can also be regarded as a special case of dimension reduction that maps all the data points into the label value space. The label error of y_i is defined as $err_{li} = s_i \|y_i - f_i\|^2$, where s_i is the flag to identify the

labeled points satisfying $s_i = \begin{cases} 1 & \dots & i \in L \\ 0 & \dots & i \notin L \end{cases}$, L is the collection of indices of labeled points, and

$F = [f_1, \dots, f_n]$ is the given label value. The loss function $Err_p(Y)$ defined on weighted combination of point approximation error and label error and its optimal solution Y^* are shown in (4).

$$Err_p = \sum_{i=1}^n \left((1-a_i)^2 err_{pi} + a_i^2 err_{li} \right) = \|YB_p(I_n - A)\|_F^2 + \|(Y - F)A\|_F^2, \quad (4)$$

$$Y^* = FAA^T (M_p + AA^T)^{-1}$$

where $Y^* = FAA^T (M_p + AA^T)^{-1}$, $a_i = (\frac{l}{n}(1-a^0) + a^0)s_i$ is the weight coefficient at y_i , l is the number of labeled points, a^0 is the minimal weight coefficient set by user, and $A = \text{diag}(a_i)$. Here, the setting of the weight coefficient a_i is based on the following two assumptions that: if the proportion of the labeled points decreases, we have to reduce our dependence on the knowledge only retained from the labeled points; if all the points are labeled, we must totally discard the geometric knowledge of the point clouds, for the label information is more reliable and the geometric knowledge is completely useless at that moment.

Similarly, the total error defined for block approximation and its optimal solution are

$$\begin{aligned} Err_b &= \sum_{i=1}^n \left((1-a_i)^2 err_{bi} + a_i^2 err_{li} \right) = \|YS_b B_b (I_K - A_b)\|_F^2 + \|(Y-F)A\|_F^2, \\ \text{optimal } Y^* &= FAA^T (M_b + AA^T)^{-1} \end{aligned} \quad (5)$$

Here, $M_b = S_b B_b (I_K - A_b)(I_K - A_b)^T B_b^T S_b^T$, $K = k \times n$, $A_b = \text{diag}\{a_1 I_k, \dots, a_n I_k\}$ is a sparse weight matrix. We take $y^0 = \frac{1}{n-l} \sum_{i \notin L} y_i$ as the decision threshold for classification.

Medical DR Image Alignment computation issues

The drawback of the algorithm presented before is that it involves the operations of large sparse matrix. Some methods are presented here to reduce the complexity of the computation. The manifold constraint matrix M of each dataset can be computed by

$$M(\bar{\Gamma}_i, \bar{\Gamma}_i) \leftarrow M(\bar{\Gamma}_i, \bar{\Gamma}_i) + W_i, \quad i = 1, \dots, n \quad (6)$$

with initial $M = 0_{n \times n}$ [4]. Let $\tilde{\Gamma}_j$ denote the vector of indices of T_j in the global coordinates \tilde{T} , n_j denote the number of points in dataset T_j , and \tilde{n} be the number of points in \tilde{T} . Let $\tilde{n}_c = \sum_{j=1}^m n_j$ denote the number of equation constraints of all datasets. By aligning the equation constraints in each dataset, we can get the total manifold constraint matrix.

$$\tilde{M}(\tilde{\Gamma}_j, \tilde{\Gamma}_{c_j}) = M_j, \quad j = 1, \dots, m \quad (7)$$

with initial $\tilde{M} = 0_{\tilde{n} \times \tilde{n}_c}$. Here, $\tilde{\Gamma}_{c_j} = \left[\sum_{k=1}^{j-1} n_k + 1 \quad \dots \quad \sum_{k=1}^j n_k \right]^T$ is the index of the manifold constraints of Y_j in the total constraints. The total manifold constraint matrix can be computed by

$$\tilde{B} = \tilde{M} \tilde{M}^T \quad (8)$$

Experiments and discussion

We validate the effectiveness of our algorithms by solving the problem of image sequence alignment. The images of two objects in COIL20 are shown in Figure 1. The images of the objects were taken at pos intervals of 5 degrees.

The embedded manifolds before aligned are shown in Figure 2, and the embedded manifolds after aligned are shown in Figure 3. The matching points for aligning the manifold of different image sequences are marked as large dots by different colors (red, white, black). We can see that our algorithms can align the embedded manifolds properly with the knowledge extracted from the matching points and the relationship among points of each image sequence.

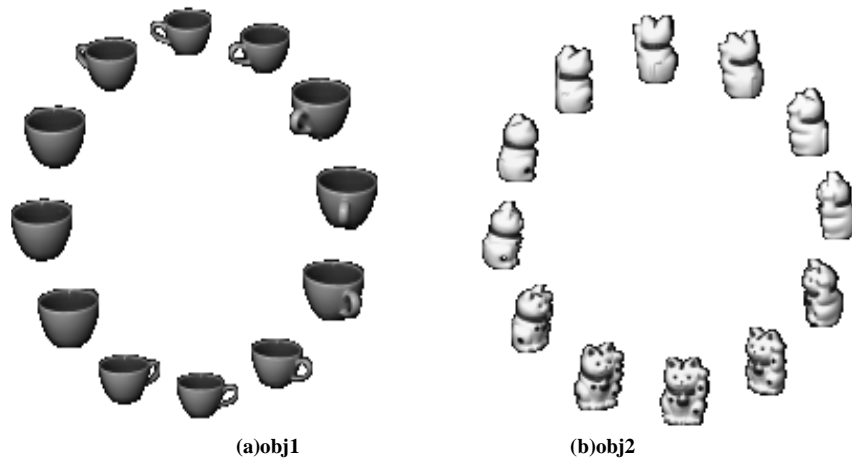


Figure 1. Images of Two Objects in COIL20

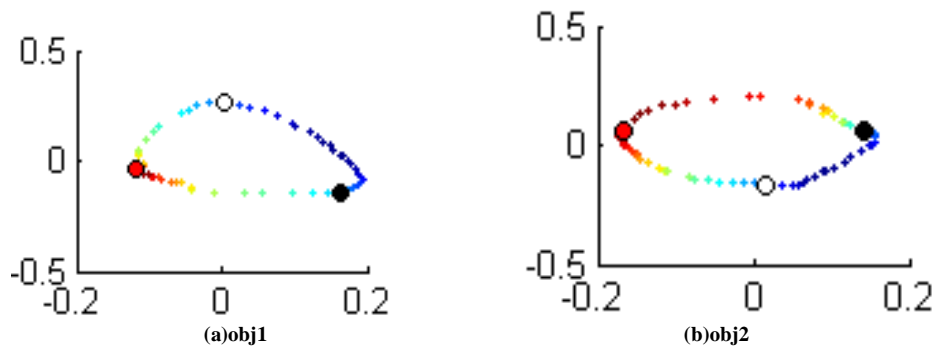


Figure 2 Embedded Manifolds Before Aligned

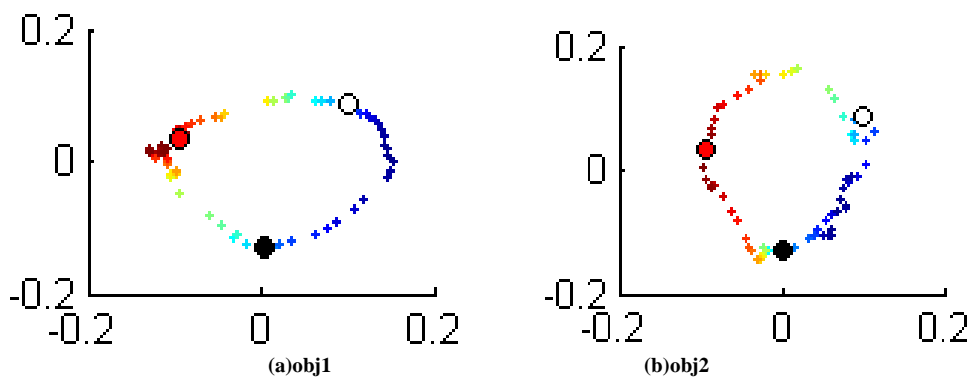


Figure 3. Embedded Manifolds After Aligned

We also select two image sequences for experiments from the FacePix database[8][9]. The image sequences corresponding to the profile view of the object taken with the camera placed at 90 degrees from the frontal are shown in Figure 4. The embedded manifolds before aligned are shown in Figure 5, and the embedded manifolds after aligned are shown in Figure 6.

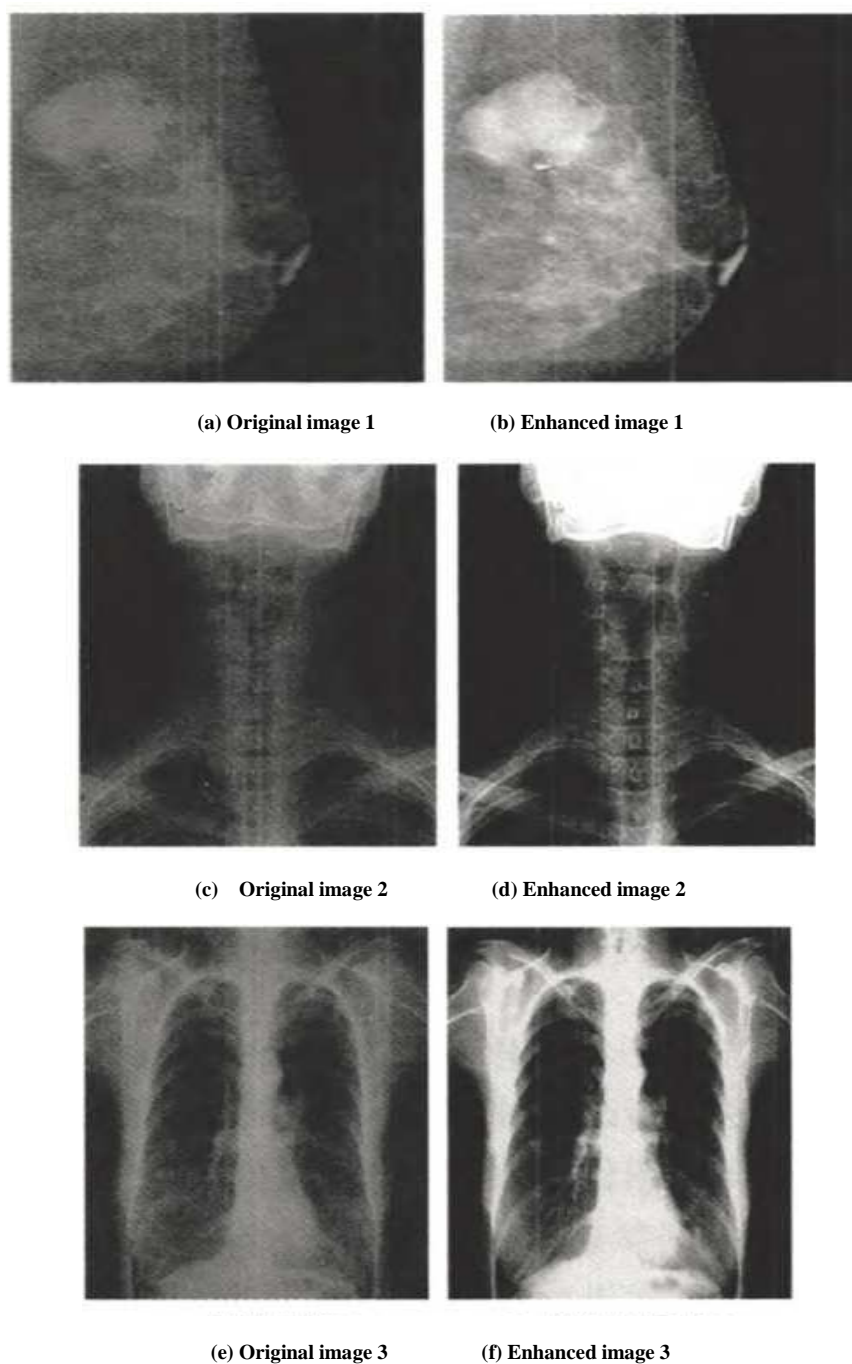


Figure 4. Enhancement contrast of DR image

CONCLUSION

In this work, we introduced improved tangent space algorithm to solve medical DR image alignment problem. Our algorithm does not need the same guarantees of global optimality or convergence, it also does not involve many more free parameters, such as learning rates, convergence criteria, or architectural specifications. The experiment result of aligning image sequences validates the effectiveness of our algorithm.

Acknowledgments

This paper is supported by Scientific Research Fund of Hunan Provincial Education Department (Grant no.12B023).

REFERENCES

- [1] J.Ham; D.Lee; L.Saul, Proc. 10th Int'l Workshop Artificial Intelligence and Statistics, page 120-127, **2005**.
- [2] A.P.Shon; K.Grochow; A.Hertzmann; R.Rao, In Proc. NIPS, page 1233-1240, **2006**.
- [3] S.Lafon; Y.Keller; R.R.Coifman, *IEEE PAMI*, 28(11): 1784-1797, **2006**.
- [4] Z.Zhang; H.Zha, *SIAM J. Sci. Comput.* 26 (1): 313-338, **2004**.
- [5] X.Bai; H.Yu; E.R , Proc. Int'l Conf. Pattern Recognition, page 398-401, **2004**.
- [6] M.Gori; M.Maggini; L.Sarti, *IEEE PAMI*, 27(7): 1100-1111, **2005**.
- [7] Y.Keselman; A.Shokoufandeh; M.F.Demirci; S.J. Dickinson, Proc. Conf. Computer Vision and Pattern Recognition, page 850-857, **2003**.
- [8] J.Black; M.Gargasha; K.Kahol; P.Kuchi; S.Panchanathan, ITCOM, Internet Multimedia Systems II, Boston, July **2002**.
- [9] G.Little; S.Krishna; J.Black; S.Panchanathan, ICASSP **2005**, Philadelphia, 2005.